

# Direct Observation of (110), (100) and (211) Facets on $^3\text{He}$ Crystals

V. Tsepelin, H. Alles, A. Babkin<sup>a</sup>, J.P.H. Härme, R. Jochemsen<sup>b</sup>,  
A.Ya. Parshin<sup>c</sup> and G. Tvalashvili<sup>d</sup>

*Low Temperature Laboratory, Helsinki University of Technology,  
P.O. Box 2200, FIN-02015 HUT, Helsinki, Finland*

<sup>a</sup>*Department of Physics and Astronomy, University of New Mexico,  
800 Yale Boulevard NE, Albuquerque NM 87131, USA*

<sup>b</sup>*Kamerlingh Onnes Laboratory, Leiden University, P.O. Box 9504,  
2300RA Leiden, The Netherlands*

<sup>c</sup>*P.L.Kapitza Institute for Physical Problems, ul. Kosygina 2,  
117334 Moscow, Russia*

<sup>d</sup>*Department of Physics, Lancaster University, Lancaster LA1 4YB, UK*

*We present the results of our recent observations on  $^3\text{He}$  crystals grown from the superfluid phase at 0.55 mK. The crystal images were obtained with a low-temperature multiple-beam interferometer. The angles between the crystal facets were measured by employing a phase-shift technique and true 3D shapes of the crystals were reconstructed on the basis of the obtained information. Three different types of facets (110), (100) and (211) were clearly visible in these experiments.*

*PACS numbers: 67.80.-s, 68.45.-v, 68.35.Rh, 42.87.Bg.*

## 1. INTRODUCTION

Morphology of  $^3\text{He}$  crystals has been studied by several groups using optical methods<sup>1,2</sup>. In these experiments three types of facets (110), (100) and (211) were identified by analyzing two-dimensional projections of the facet's edges<sup>2</sup>. In this paper we present our new results of direct observations of the different facet types on  $^3\text{He}$  crystals obtained using interferometric techniques and reconstruction of the 3-dimensional crystal shape.

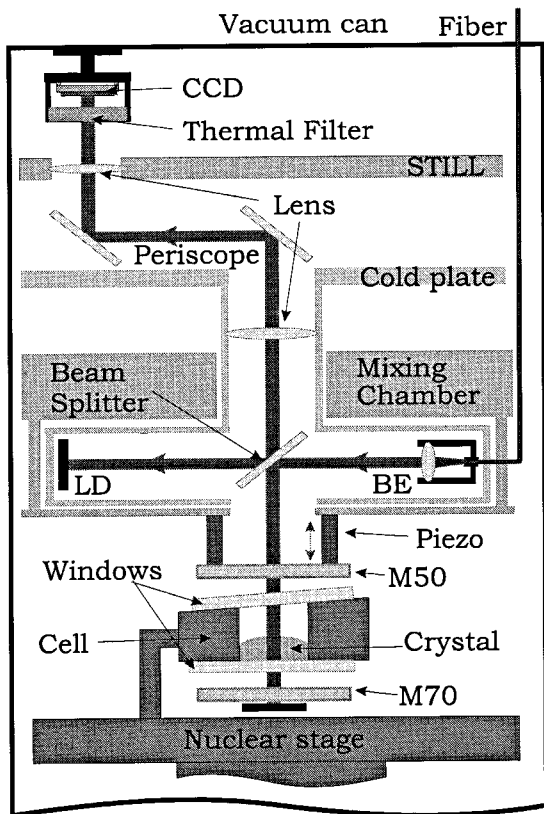


Fig. 1. General scheme of the optical setup. (LD - light dumper, BE - beam expander). For details, see text.

## 2. EXPERIMENTAL SETUP

Interferometric studies of the  $bcc$ - ${}^3\text{He}$  crystals require the use of path interferometry which allows simultaneous observation of the global crystal shape and of the fine details of the solid/liquid interface. Based on our experience with optical studies<sup>3</sup> on various helium interfaces, we have developed a novel setup which utilizes a Fabry-Pérot type of interferometry with a phase-shift facility (see fig. 1).

A nuclear demagnetization cryostat is used to cool down the Pomeranchuk-type experimental cell which contains  $13\text{ cm}^3$  of  ${}^3\text{He}$ . The  ${}^3\text{He}$  pressure is monitored by a high precision Straty-Adams gauge which is also used as melting curve thermometer<sup>4</sup>.

The optical part of the cell consists of a cylindrical copper body ( $\phi = 16$  mm,  $h = 12$  mm) which is sealed off by two antireflection-coated fused-silica windows. A multiple-beam interferometer is formed by two parallel mirrors with 50% (M50) and 70% (M70) reflectivities above and below the cell. Both mirrors are thermally anchored to the mixing chamber of the dilution refrigerator. The upper mirror can be moved in vertical direction by means of a cylindrical piezo-electric crystal to which the mirror is attached. Placed just outside the field of view is a sharp tungsten-metal tip nucleator to which a high voltage can be applied.

A He-Ne laser beam ( $\lambda = 632.8$  nm) is guided through a single mode fiber into the vacuum jacket where the beam expander (BE) expands it to a diameter of 8 mm. Via a 50% beam splitter the beam enters the interferometer through the upper mirror (M50). The light undergoes multiple reflections between the mirrors and the interference pattern, formed by the interfering beams, is reflected back through the upper mirror. A system of lenses and periscope focuses it to a cooled CCD sensor which has  $575 \times 383$  elements (pixels). Our horizontal resolution is one pixel, corresponding with  $15.3 \pm 0.4$   $\mu\text{m}$ . Crystal surfaces with a slope of up to 60 degrees with respect to the direction of the illumination can be measured.

### 3. MEASUREMENT TECHNIQUE AND DATA ANALYSIS

Figure 2a shows an interferogram of a  $^3\text{He}$  crystal at 0.55 mK during relaxation. This crystal was nucleated from the B-phase of superfluid  $^3\text{He}$  by applying a high voltage pulse to the nucleator when the liquid pressure was slightly above the melting curve<sup>5</sup>. The background pattern that dominates the center and the right part arises from the liquid helium wedge (due to the  $2^\circ$ -tilt of the upper window) and nonparallelity of the mirrors. The crystal shows up in the left part of the interferogram. The regions with equidistant parallel fringes in the crystal part of the interferogram correspond to flat surfaces (planes) on the crystal.

In principle it is possible to determine a crystal shape from a single interferogram using intensity based analysis methods. First, the positions of the fringe minima have to be located and combined to a skeleton pattern. Secondly, the fringe ordering problem has to be solved and the minima have to be combined to a three-dimensional surface.

However, the phase of a wavefront can be directly calculated from the changes in the recorded intensity data when a known phase change is induced by modifying the mirror distance in the Fabry-Pérot interferometer. The precision of this method is significantly higher than digitizing the fringe

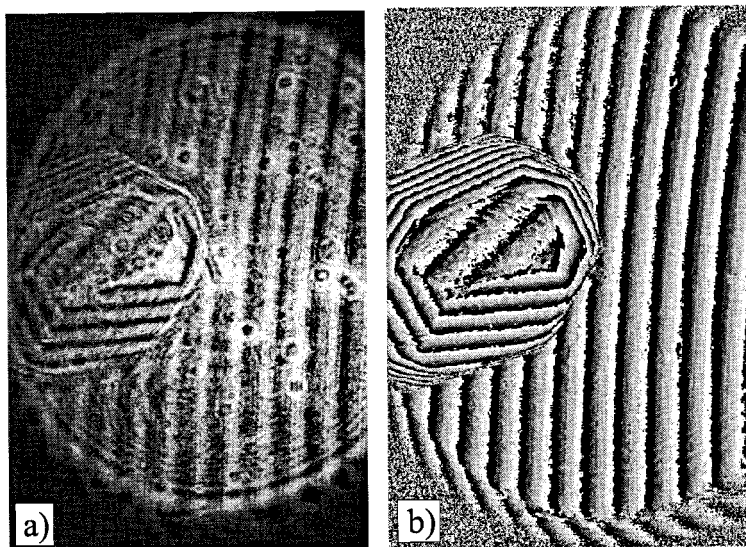


Fig. 2. a) The interferogram of a  $^3\text{He}$  crystal at 0.55 mK during relaxation and b) the corresponding phase map measured using phase-shift technique.

positions.

We have measured the wavefront phase using the following technique<sup>6,7</sup>: four subsequent interferograms were taken with a  $\pi/2$  phase shift in between; the optical path was changed by applying a high voltage to the piezo crystal. From these four interferograms ( $I_1$ ,  $I_2$ ,  $I_3$  and  $I_4$ ) the wrapped phase  $\varphi_w$  (the phase modulo  $2\pi$ ) was calculated using the formula

$$\varphi_w = \frac{1}{2} \arcsin \frac{(I_1 - I_3)(I_2 - I_4)}{(I_1 - I_2)(I_3 - I_4) + (I_2 - I_3)(I_4 - I_1)}.$$

Figure 2b shows the result of the phase measurement of the same  $^3\text{He}$  crystal shown in fig. 2a.

The removal of phase ambiguities (modulo  $2\pi$ ) was obtained by a standard image processing technique, called phase unwrapping<sup>8</sup>. Once the continuous (unwrapped) phase  $\varphi$  is known, the crystal thickness  $d$  can be calculated by

$$d = \frac{\lambda}{4\pi\Delta n} \varphi,$$

where  $\Delta n = 1.66 \cdot 10^{-3}$  is the difference in refractive indices of solid and liquid  $^3\text{He}$  at about 1 mK. The thickness profile corresponds to the real shape of the crystal when the bottom of the crystal is a single flat surface.

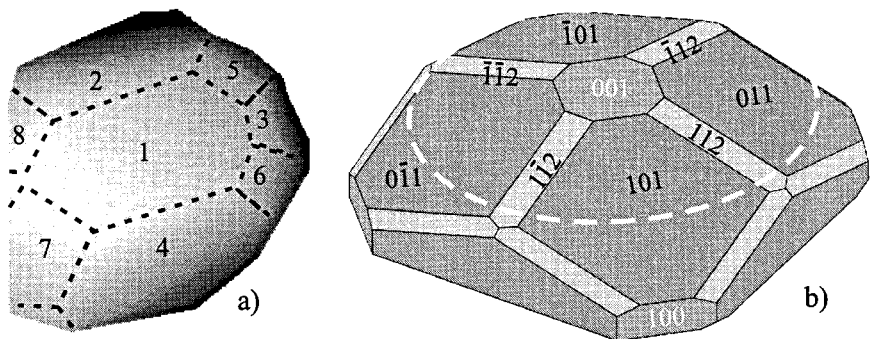


Fig. 3. a) Unwrapped phase of the  $^3\text{He}$  crystal. b) Computer generated shape of a *bcc*-crystal with three different facet types.

Figure 3a illustrates the unwrapped phase of the  $^3\text{He}$  crystal shown in fig. 2 (the dotted line marks the edges between different flat regions). First each flat area was selected (see table 1 column 1) and fitted with a plane. Then the normals to the planes were found and a conversion to physical dimensions was carried out. After that the angles between different flat regions were calculated.

Next the structure of the crystal surface was resolved. The angles between the central and the neighboring planes were compared with theoretical angles for the (perfect) *bcc*-structure and a guess for the facet types was done. After that the angles between all facets were cross-checked. The second column of table 1 shows the measured and corresponding calculated angles for plane '1' versus the other planes. The angles for 101 and 112 facets which are used to check the consistence of identified facets are listed in the next two columns. The last two columns of the table show the identified facets and their type.

The estimated error of the angle measurements is approximately  $1.2^\circ$  which is twice as small as the largest observed difference between the expected and measured angles. A possible reason for this discrepancy can be non-parallel vertical movement of the upper mirror and/or the change of the horizontal scale which was calibrated at room temperature.

Figure 3b shows the numerically calculated surface profile of the ideal *bcc*-crystal with (110), (100) and (211) types of facets. The Miller indices for each facet are presented. The top of the generated crystal surface is marked by a white dashed line to illustrate which part of the crystal observed in the experiment.

Table 1. Experimentally measured and theoretically calculated angles between different types of facets.

plane	1		4		6		facet	facet type
	exp	calc	exp	calc	exp	calc		
1	-	-	47	45	38	35.3	001	< 100 >
2	44	45	63	60	75	73.2	$\bar{1}01$	< 110 >
3	47	45	-	-	29	30	011	
4	45	45	59	60	29	30	101	
5	36	35.3	32	30	49	48.2	$\bar{1}12$	< 211 >
6	38	35.3	29	30	-	-	112	
7	34	35.3	74	73.2	50	48.2	$1\bar{1}2$	
8	34	35.3	74	73.2	72	70.5	$\bar{1}\bar{1}2$	

#### 4. CONCLUSIONS

We studied morphology of  $^3\text{He}$  crystals at 0.55 mK using a new optical setup. The facet types with the highest roughening transition temperatures, namely (110), (100) and (211), were clearly observed in our experiments. The identification of the facets is quite reliable as compared to previous experiments<sup>2</sup> due to the direct measurement of the wavefront phase.

#### ACKNOWLEDGMENTS

This work was supported by INTAS and EU's Large Scale Facility grants ULTI (HCM Programme) and ULTI II (TMR Programme).

#### REFERENCES

1. E. Rolley, S. Balibar and F. Gallet, *Europhys. Lett.*, **2(3)** (1986) 247.
2. R. Wagner *et al.*, *Phys. Rev. Lett.* **76** (1996) 263.
3. P. Hakonen *et al.*, *J. Low Temp. Phys.* **101** (1995) 41 and references therein.
4. W. Ni *et al.*, *JLTP* **101** (1995) 305.
5. V. Tsepelin *et al.*, *Physica B* **284-288** (2000) 351.
6. G. Bönsch, H. Böhme, *Optik* **82** (1989) 161.
7. J.P.H. Härme *et al.*, *Physica B* **284-288** (2000) 349.
8. D.W. Robinson and G.T. Reid, *Interferogram Analysis*, IOP Publishing Ltd., 1993.